Design and Synthesis of Chemiluminescent Cassettes Based on Energy Transfer

Steven Vertueux, Alexandre Haefele, Kathleen Solmont, Philippe Durand, Pierre-yves Renard

EurJOC
European Journal of Organic Chemistry

Research Article
doi.org/10.1002/ejoc.202201401

Chemistry Europe
European Chemical Societies Publishing

www.eurjoc.org

Special Collection

Design and Synthesis of Chemiluminescent Cassettes Based on Energy Transfer

Steven Vertueux,[a] Alexandre Haefele,*[a] Kathleen Solmont,[a] Philippe Durand,[b] and Pierre-Yves Renard*[a]

Chemiluminescent probes are being considered as a convenient option for optical imaging. Several strategies were reported to increase the probe chemiluminescence efficiency. In this study, a series of chemiluminescent cassettes based on adamantyl stabilized 1,2-dioxetanes ("Schaap's dioxetane") linked to a fluorophore (BODIPY or dicyanoisophorone fluorophore) by a conjugated linker have been synthetized. Their chemiluminescent decomposition and the photoluminescence properties of their respective emissive species were investigated.

Introduction

Amongst optical imaging tools used in medical imaging, chemiluminescence offers high signal-to-noise ratio due to the absence of excitation light.[1] Recent examples have shown that chemiluminescent probes could be used not only to detect oxidative processes, but also to probe enzymatic activities.[2] Yet, the energy required for photon emission comes from the strain release obtained through the ring opening of a highly unstable intermediate. Adamantylidene-1,2-dioxetane moiety (Schaap's dioxetane)[3] attached in meta position to a phenol appears as one of the best candidates because it does not require any oxidation step to release a photon, the dioxetane decomposition being initiated by the formation of the phenolate ion. This chemiluminescence triggering mechanism associated with a stable dioxetane ring in absence of a triggering anion in the meta position of the attached aromatic moiety allows this family of chemiluminescent probes to be used to detect a wide range of chemical and biological analytes.[4,5] Schaap's dioxetane activation mechanism is depicted in Scheme 1. Firstly, the phenolate formation triggers the so called *Chemically Initiated Electron Exchange Luminescence CIEEL* which allows the decomposition of the four membered ring and generates an excited species which emits a photon.[6,7] Yet, this scaffold suffers from a low chemiluminescence quantum yield in aqueous conditions (often less than 0,01 %), and an emission wavelength too far below the 650–850 nm optimal NIR optical in vivo imaging window.[8] Moreover, a micellar enhancer is required to limit chemiluminophore quenching interactions with water molecules and green shift the emission wavelength, thus limiting the applications of chemiluminescence for in vivo biological imaging.[9] Therefore, several strategies were implemented to improve the compatibility of this chemiluminescent scaffold to bioimaging applications. The first strategy implemented to improve the chemiluminescence efficiency was to design "energy transfer cassettes". Cassettes are molecular entities in which an energy transfer occurs between an energy donor and an acceptor to red-shift the emission wavelength.[10] In this case, a chemiluminophore (donor) is linked to a fluorophore (acceptor) and issues indirect chemiluminescence (Scheme 2A). This can be achieved via through space energy transfer (named CRET for *Chemiluminescence Resonance Energy Transfer*) to an emissive fluorophore in water.[11–13] However, this energy transfer is distance dependent between the chemiluminescent platform (the phenol core) and the fluorophore. Moreover, space orientation of the couple has also an influence on the final emission efficiency, and the fluorophore emission range is limited by the chemiluminophore emission/fluorophore excitation overlap required for efficient CRET.[14] More recently, Shabat et al.[15,16] provided a real breakthrough by designing a push pull system directly on the phenol core (Scheme 2B), with an increased chemiluminescence quantum yield and redshifted emission. Another possibility for indirect chemiluminescence is to design more rigid cassettes where the chemiluminophore is attached to a fluorophore by a conjugated linker. In this case, the energy transfer process is considered to be faster than the Förster Resonance Energy Transfer (FRET), and does not require a donor emission/acceptor excitation overlap.[17,18] This type of transfer was already successfully achieved by using luminol as the chemiexcited part, and red emitting fluorophores.[19,20] To expand the scope of this strategy we wish to describe in this communication, the synthesis of such chemiluminophores based on Schaap's

[a] S. Vertueux, Dr. A. Haefele, Dr. K. Solmont, Prof. P.-Y. Renard
Normandie Univ, UNIROUEN
INSA Rouen, CNRS, COBRA (UMR 6014)
1 rue Tesnière, 76821 Mont-Saint-Aignan Cedex (France)
E-mail: alexandre.haefele@univ-rouen.fr
pierre-yves.renard@univ-rouen.fr
[b] Dr. P. Durand
Université Paris-Saclay, CNRS
Institut de Chimie des Substances Naturelles, UPR 2301
91198, Gif-sur-Yvette (France)

Supporting information for this article is available on the WWW under https://doi.org/10.1002/ejoc.202201401

Part of the "LabEx SynOrg" Virtual Institute Feature.

Research Article
doi.org/10.1002/ejoc.202201401

Chemistry Europe
European Chemical Societies Publishing

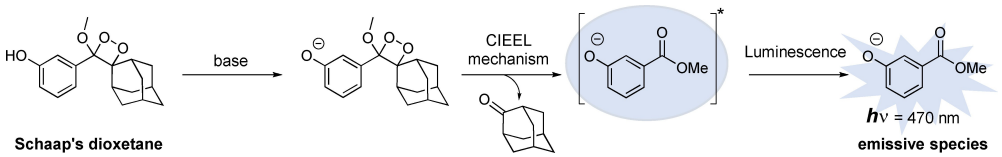

Scheme 1. 1,2-dioxetane based Schaap's probe activation mechanism.

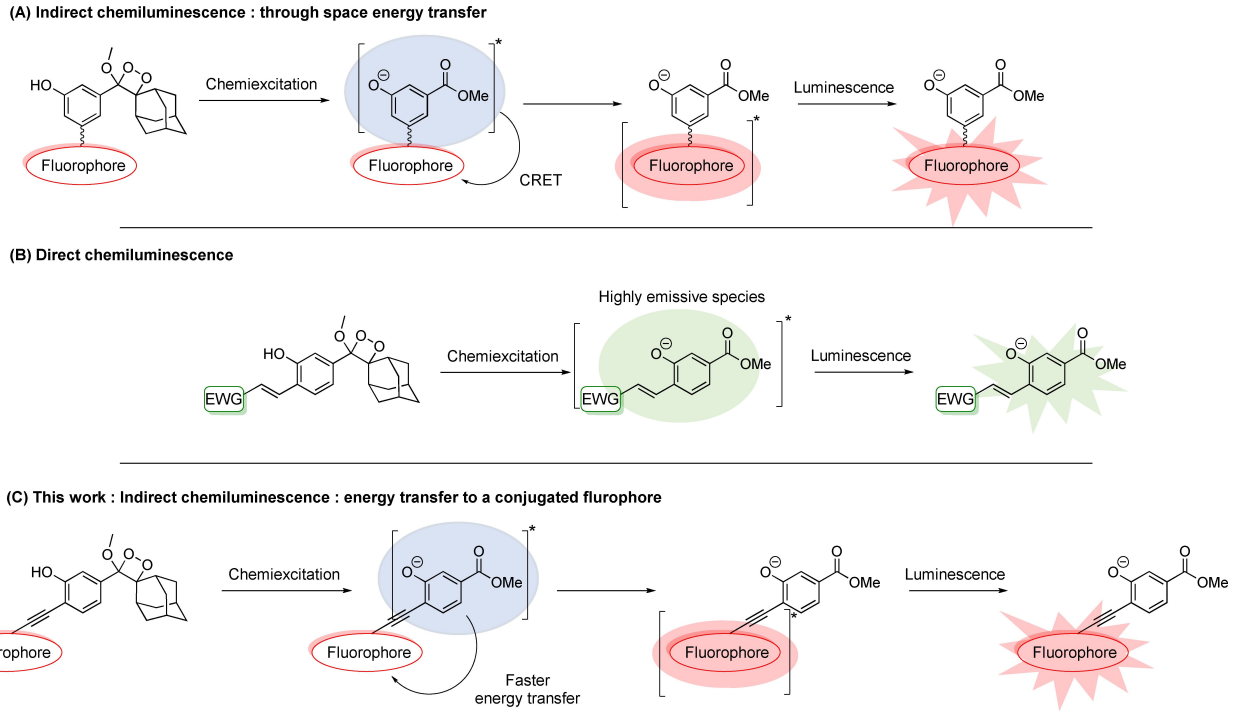

Scheme 2. Implemented strategies to enhance the efficiency of 1,2-dioxetane based chemiluminescent probes and to redshift the emission wavelength **(A)** indirect chemiluminescence via CRET, (B) direct chemiluminescence with enhancement of the chemiluminescence quantum yield via a substituent effect or **(C)** indirect chemiluminescence via transfer to a conjugated fluorophore.

dioxetane, directly conjugated to a red emitting fluorophore (Scheme 2C). During the writing of this manuscript, Lippert et al. described a first example of an Ir(III) complex directly attached to a chemiluminescent motif.[21]

Results and Discussion

By analogy with the chemiluminescent cassettes described with luminol as the chemiexcited moiety and to evaluate the potential of such chemiluminescent energy transfer strategy, we designed three different targets (Figure 1). Two of them display a BODIPY based fluorophore (in a first intent, we chose 1,3,5,7 tetramethyl BODIPY, emitting at 520 nm as a model BODIPY), attached on the phenyl of Schaap's dioxetane either directly (**BDP-CL**), or through a conjugated alkyne linker (**E-BDP-CL**). The third target displays a dicyanoisophorone (DCI) based fluorophore (emission centered at 702 nm) conjugated to the Schaap's dioxetane also through an alkyne linker (**DCI-CL**).

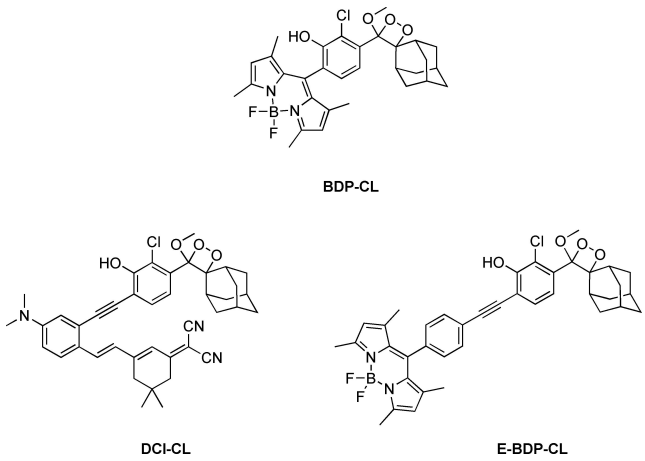

Figure 1. Chemiluminophores synthetized in this work.

Research Article
doi.org/10.1002/ejoc.202201401

Chemistry Europe
European Chemical Societies Publishing

Chemiluminophore synthesis

BODIPY-phenol dioxetane **BDP-CL** was synthesized from aldehyde **1**[22] as described on Scheme 3. The phenol was first protected as an *o*-nitrobenzyl ether. This photo-labile protective group was used in order to offer mild and neutral deprotection conditions. Then, dipyrromethane **3** was generated by a condensation with two equivalents of 2,4-dimethylpyrrole with a good 86% yield. BODIPY **4** was synthetized with a two-step one-pot procedure with 30% yield, consisting in DDQ mediated oxidation of **3** into dipyrromethene followed by boron complexation using $BF_3.Et_2O$ in presence of Et_3N in toluene. Phenol **5** was obtained by photocleavage of the *o*-nitrobenzyl ether under UV light and acidic conditions. It was further converted into the final chemiluminophore **BDP-CL** via a [2 + 2] photocycloaddition with singlet oxygen generated in situ using methylene blue as photosensitizer. Despite a full conversion of the starting material **5**, the apparent sensitivity of the dioxetane **BDP-CL** to silica gel led to a moderate yield of 50% after purification.

Chemiluminophore **E-BDP-CL** was synthesized from iodophenol **6** as described in Scheme 4. The phenol function was also first protected as an *o*-nitrobenzyl ether. The ethynyl link in compound **9** was then formed via a Sonogashira cross-coupling reaction between protected iodophenol **7** and ethynyl-BODIPY **8**, which was synthetized according to known procedures.[23] To avoid any Glaser coupling by-product, the reaction mixture must be carefully deoxygenated with a freeze-pump-thaw procedure. After photocleavage of the *o*-nitrobenzyl moiety, the phenol derivative **10** was engaged in a [2 + 2] photocycloaddition with singlet oxygen, as described for **BDP-CL**, to form the final dioxetane **E-BDP-CL**. The latter seems more stable than the dioxetane **BDP-CL** and was obtained with 80% yield, after purification on silica gel.

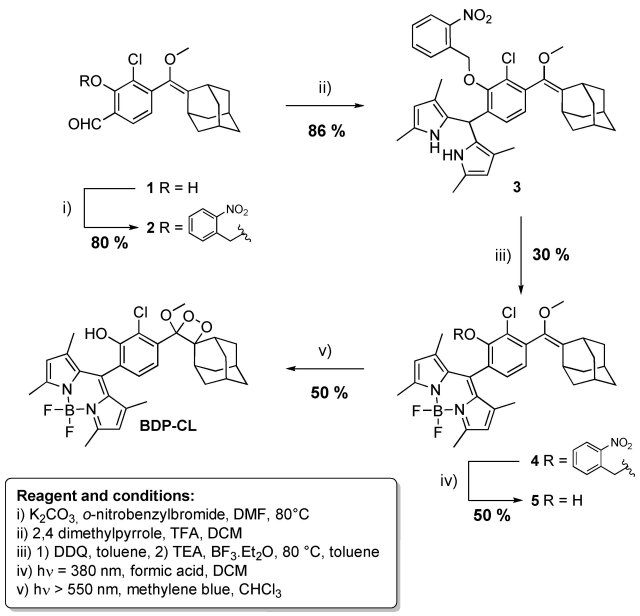

Scheme 3. Chemiluminophore **BDP-CL** synthesis.

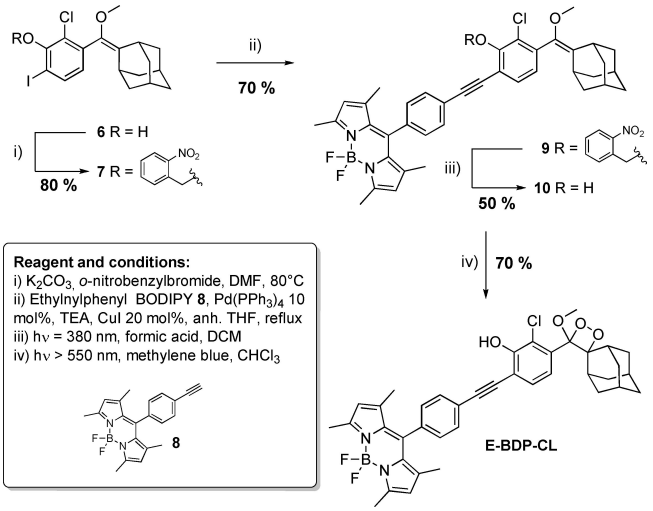

Scheme 4. Chemiluminophore **E-BDP-CL** synthesis.

The third chemiluminophore **DCI-CL** was obtained as described in Scheme 5 from benzaldehyde **11**. DCI fluorophore **15** was prepared in three steps using adapted literature procedures[24] in order to introduce an alkyne linker. The protected alkyne **12** was obtained through a Sonogashira cross coupling reaction with ethynyl-TMS and was then involved in a Knoevenagel condensation with dicyano derivative **13** in presence of piperidine and a catalytic amount of acetic acid to form DCI fluorophore **14**. To avoid the double bond photoisomerization, the reaction mixture was protected from light. Removal of the trimethylsilyl group using Tetrabutylammonium fluoride (TBAF) at 0 °C in THF afforded DCI fluorophore **15** with 80% yield. In this synthesis, iodophenol **6** was protected as silylether **16** and was engaged in a copper free Sonogashira reaction with **15** using Tetrakis(triphenylphosphine)palladium as palladium (0) source. Indeed, the freeze-pump-thaw procedure proved to be not efficient enough to avoid the formation of Glaser coupling by-product, thus copper had to be removed from the reaction process. Finally, chemiluminophore **DCI-CL** was obtained with a moderate 36% yield over two steps, by deprotection of phenol **17**, with TBAF in THF at 0 °C, followed by a [2 + 2] photo-cycloaddition with singlet oxygen using the same conditions as before.

Chemiluminescence results

Chemiluminescence spectra were recorded in DMSO with the addition of a small amount of basic phosphate buffer (PBS 0.01 M pH = 11.6) to trigger the CIEEL mechanism by formation of the phenolate through deprotonation of the phenol moiety (Figure 2). Each chemiluminescent assay was controlled by RP-HPLC (see Figure S1 in Supporting Information). All three chemiluminophores gave very weak emission signals under these conditions with CL quantum yields in the order of 10^{-3} (see Table 1 and Supporting Information for details). Chemiluminophore **BDP-CL** gave such a weak luminescence that we

Research Article
doi.org/10.1002/ejoc.202201401

Chemistry Europe
European Chemical Societies Publishing

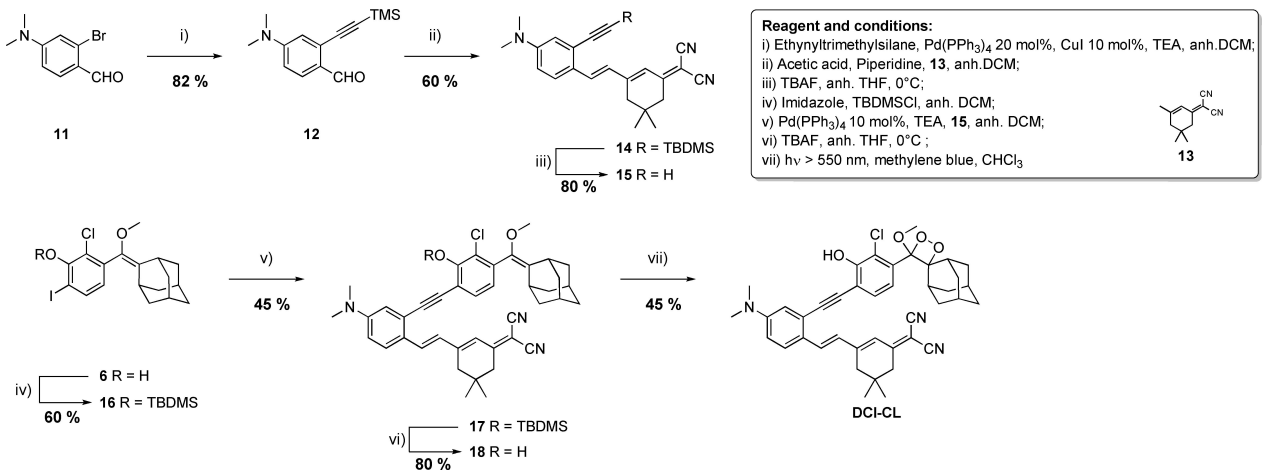

Scheme 5. Chemiluminophore **DCI-CL** synthesis.

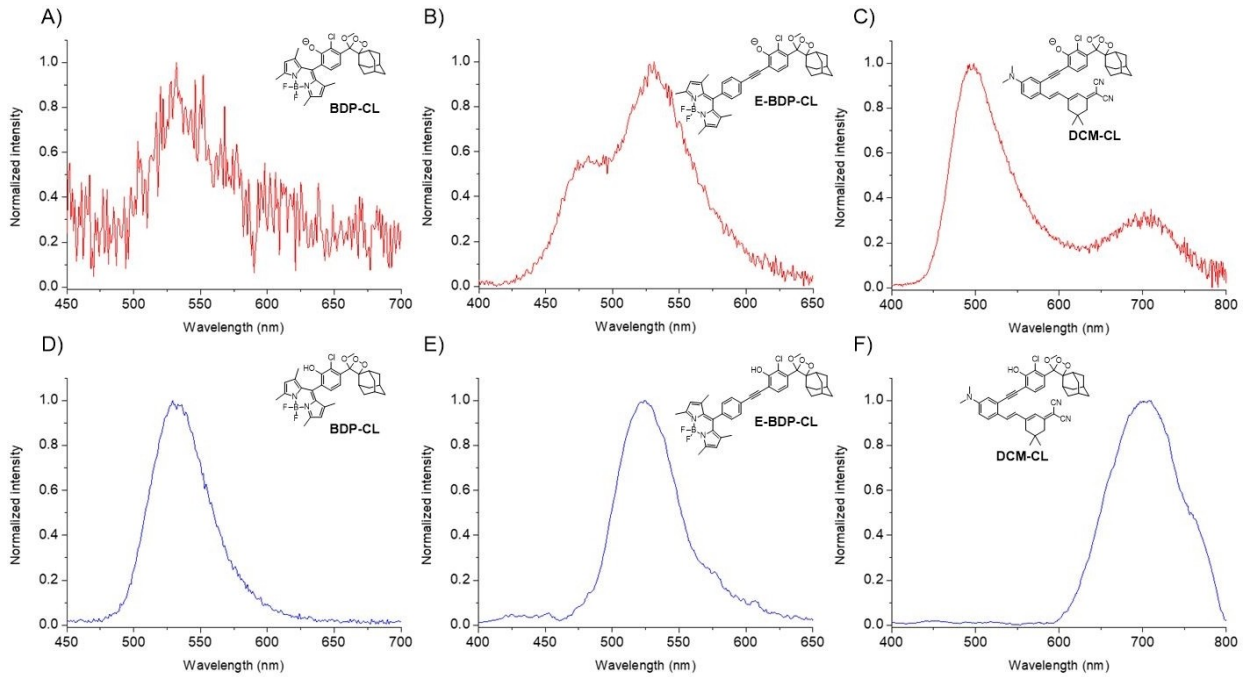

Figure 2. Chemiluminescence spectra (red lines, conditions: room temperature in 2 mL of DMSO upon addition of 100 μL of 0.01 M PBS pH 11.6 buffer, concentrations: A) 5 μM, B) 49 μM and C) 68 μM) and thermoluminescence spectra (blue lines, conditions: 2 mL of DMSO at 100 °C with 50 μL of PBS buffer 0.01 M pH 1.2, concentrations: D) 23 μM, E) 10 μM and F) 142 μM) of dioxetanes **BDP-CL**, **E-BDP-CL** and **DCI-CL.** *Thermoluminescence spectra of **E-BDP-CL** and **DCI-CL** were smoothed with the origin software: 36 pts FFT smooth.

were not able to get a reliable emission maximum for the recorded emission profile (Figure 2A). Chemiluminescence profile of **E-BDP-CL** displays two emission maxima around 488 and 530 nm respectively. The first emission band can be attributed to Schaap's dioxetane direct chemiluminescence (reported at 470 nm in DMSO,[3] the small red shift to 488 nm can be attributed to the conjugated ethynyl moiety), whereas the emission centered at 530 nm can be attributed to the BODIPY core[25] (Figure 2B). The same profile was observed for **DCI-CL** with a large gap between the two maxima, centered at 495 and 704 nm (Figure 3C). According to the CIEEL mechanism, the phenolate formed under the reaction conditions is the emissive species. In order to understand the reason of these very weak intensities, we investigated whether it could be linked to an interaction between this negative charge and the fluorophore. Thus, chemiluminescence spectra from the thermal decomposition of the three probes, which will be called thermoluminescence, were recorded in DMSO (100 °C) with a small amount of acidic phosphate buffer (PBS 0.01 M pH = 1.2) to ensure the complete phenol protonation. Under these conditions, all chemiluminophores displayed only one emission band, centered at 533, 527 and 704 nm for **BDP-CL**, **E-BDP-CL** and **DCI-**

Research Article
doi.org/10.1002/ejoc.202201401

Table 1. Photoluminescence (PL), Chemiluminescence (CL), and Thermoluminescence (TL) data.

Compound	Under acidic conditions λ^{max}_{em} [nm]	Under basic conditions λ^{max}_{em} [nm]	Quantum yield Φ_{CL} ($\times 10^{-3}$)[c]
BDP-CL	$\lambda_{TL}=529$	n.d.	1.78
19	$\lambda_{PL}=523$[a]	n.d.	–
E-BDP-CL	$\lambda_{TL}=528$	$\lambda_{CL}=479, 528$	4.10
20	$\lambda_{PL}=523$[a]	$\lambda_{PL}=479, 519$[a]	–
DCI-CL	$\lambda_{TL}=704$	$\lambda_{CL}=495, 704$	28.7
21	$\lambda_{PL}=704$[b]	$\lambda_{PL}=495, 704$[a]	–

[a] $\lambda_{ex}=400$ nm; [b] $\lambda_{ex}=520$ nm; [c] measured in DMSO with unsubstituted chlorophenol adamantylidene dioxetane as reference ($3.2.10^{-3}$ in PBS).

CL, respectively (Figure 2). These wavelengths correspond to the respective fluorophore emission maxima, indicating that there is no detectable remaining emission from the phenol moiety and that the energy of the excited state localized on the phenol is efficiently transferred to the conjugated fluorophore. This supports our chemiluminescent cassettes design. In order to further investigate these observations, the photophysical properties of the emissive species were recorded.

Photoluminescence of the emissive species

Emissive species were isolated and characterized by ^{1}H NMR after chemiluminescence triggering on a mg scale. As expected, the three methyl esters **19**, **20**, **21** were isolated, corresponding to the 1,2-dioxetane moiety decomposition (Figure 3). Photoluminescence spectra of all three were recorded at room temperature in DMSO (phenol form) and in DMSO with the addition of basic phosphate buffer (PBS 0.01 M pH = 11.6) to get the phenolate form (Figure 3). In DMSO, both BODIPY **19** and **20** exhibit a fine and shouldered absorption band centered at 507 and 503 nm, respectively, typical of BODIPY dyes, whereas DCI displays a large and structureless absorption band with a maximum at 523 nm. With the addition of basic phosphate buffer, the lower energy absorption band of **19** is subject to a small hypsochromic shift, whereas it remained unchanged for **20** and **21**. Moreover, a new absorption band could be observed at 350, 400 and 420 nm for **19**, **20** and **21**, respectively. This band is attributed to the absorption of the phenolate moiety.[26] The photoluminescence profile of both BODIPY **19** and **20** are mirror image of the lowest energy absorption band with a small Stokes shift ($\Delta\lambda = 16$ nm) representative of the BODIPY fluorophores. DCI **21** displays a structureless emission band centered at 704 nm with a large Stokes shift ($\Delta\lambda = 181$ nm), typical of charge transfer emitters. It is worth noting that the emission maximum is redshifted by 40 nm compared to the parent DCI without the alkyne-phenol moiety.[27] Upon addition of basic phosphate buffer in the medium, the photoluminescence of all three emissive species was almost completely quenched, which is consistent with the previous observations we obtained during chemiluminescence measurements. We thus suspected the phenolate to be responsible for a fluorescence quenching phenomenon for both fluorophores.

Discussion

By overlaying both thermoluminescence and photoluminescence spectra under acidic conditions, we could confirm that the isolated esters **19**, **20** and **21** are the chemiluminescence emissive species of 1,2-dioxetane based chemiluminophores **BDP-CL**, **E-BDP-CL** and **DCI-CL**, respectively (Figure S2). The absence of residual phenol emission let us postulate that the energy of the chemiexcited phenol is efficiently transferred to the tethered fluorophore. By comparing the photoluminescence study under basic conditions with chemiluminescence assays, we could further confirm the nature of the emissive species. Indeed, the emission profile obtained for phenolates **20** and **21** upon their excitation in their absorption band at 400 nm is identical to that of the chemiluminescence produced by their respective dioxetanes **E-BDP-CL** and **DCI-CL**, although only with different relative intensities (Figure S3). This might be due to a direct excitation of the tethered fluorophore, which cannot be prevented when exciting the phenolate at 400 nm, thus increasing the intensity of the fluorophore emission. These data prove that we were able to efficiently transfer energy from the

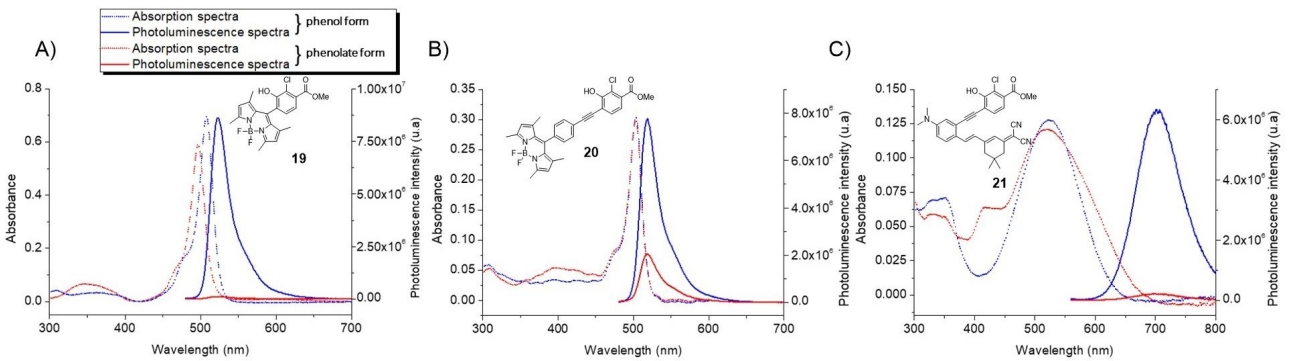

Figure 3. Absorption and emission spectra (conditions: r.t., 2 mL of DMSO (phenol form) or r.t., DMSO + 100 µL PBS buffer (0,01 M pH 11,6) (phenolate form)) A) λ_{ex}:460 nm B) λ_{ex}: 460 nm C) λ_{ex}: 520 nm of emissive species **19**, **20** and **21**.

chemiexcited phenolate moiety to different fluorophores directly linked or via a conjugated spacer at the *ortho* position of the phenolate. Nevertheless, the energy transfer was not total as a residual chemiluminescence emission of the phenolate core was observed for **E-BDP-CL** and **DCI-CL**. The fluorescence extinction observed with the phenolate species can thus be attributed to the additional electrons lone pair of the phenolate through a chemically induced electron transfer (CeT).[28–31] A literature survey revealed that BODIPY derivatives similar to **19**, with a phenol or an aniline in the pseudo *meso* position of the BODIPY core could display a fluorescence quenching by PeT under basic conditions.[32–35] These previous results lead us to conclude that such an electron transfer mechanism is responsible for the fluorescence quenching of **19** and for the weak chemiluminescence signal of **BDP-CL**. We suspect that electron transfer from the phenolate is also responsible for the fluorescence quenching of **DCI-CL** and **21** even though, to our knowledge, there is no previous study reporting PeT for DCI based fluorophores such as **DCI-CL** and **21**. Definitive evidence to confirm the chemically induced electron transfer could be obtained through additional studies such as transient UV-spectroscopy and/or spectroelectrochemistry. However, considering the low amounts of emission species and the low chemiluminescence yield we obtained, such studies are beyond the scope of this article. However, with this electron transfer hypothesis it is possible to propose a clear explanation for the weak chemiluminescence intensities. As illustrated above, once chemiexcitation has been obtained through the triggered CIEEL mechanism, thanks to the phenol deprotonation, an energy transfer takes place between the chemiexcited phenolate core and the fluorophore, together with a fluorescence quenching by a chemically induced electron transfer leading to only residual chemiluminescence.

Conclusion

In summary we achieved the synthesis of three Schaap's based 1,2-dioxetanes linked to the *ortho* position of the phenol directly or through a conjugated ethynyl linker to a BODIPY or a DCI fluorophore. Thermoluminescence assays confirmed an efficient energy transfer of the chemiexcited phenol, obtained through 1,2-dioxetane decomposition, to the conjugated fluorophore. Yet, once the phenol is deprotonated, these chemiluminophores display a weak chemiluminescence with two bands assigned to the residual chemiexcited phenolate core and to the tethered fluorophore. Photoluminescence and chemiluminescence studies allowed us to rationalize that a chemically induced electron transfer is responsible of the emission extinction for the three chemiluminophores. Further study could be done to evaluate the energy transfer quantum yield. Despite the low chemiluminescence obtained with 1,2-dioxetanes **BDP-CL**, **E-BDP-CL** and **DCI-CL**, this study paves the way for the design of efficient indirect chemiluminescent probes for bioimaging, provided that fluorophores less prone to PeT are used.

Acknowledgements

We thank Region Normandie and Labex SynOrg (ANR-11-LABX-0029) for SV PhD financial support. This work has also been partially supported by University of Rouen Normandy, the Centre National de la Recherche Scientifique (CNRS), INSA Rouen Normandy, European Regional Development Fund (ERDF), Carnot Institute I2 C and by the graduate school for research XLChem-(ANR-18-EURE-0020 XL CHEM). GDR GNRS 2037 AIM is acknowledged for a travel grant to SV.

Conflict of Interest

The authors declare no conflict of interest.

Data Availability Statement

The data that support the findings of this study are available in the supplementary material of this article.

Keywords: chemiluminescent probe · energy transfer. · indirect chemiluminescence · 1,2-dioxetane

[1] C. R. Bauer, *Imaging Microsc.* **2013**, 32–34.
[2] Y. Yang, F. Zhang, *Anal. Sens.* **2021**, *1*, 75–89.
[3] A. P. Schaap, T. Chen, R. S. Handley, *Tetrahedron Lett.* **1987**, *28*, 1155–1158.
[4] N. Hananya, D. Shabat, *Angew. Chem. Int. Ed.* **2017**, *56*, 16454–16463; *Angew. Chem.* **2017**, *129*, 16674–16683.
[5] Z. Zhan, Y. Dai, Q. Li, Y. Lv, *TrAC Trends Anal. Chem.* **2021**, *134*, 116129–116143.
[6] A. Waldemar, C. Omar, *J. Am. Chem. Soc.* **1979**, *101*, 6511–6515.
[7] J. Young Koo, G. B. Schuster, *J. Am. Chem. Soc.* **1978**, *100*, 4496–4503.
[8] R. Weissleder, V. Ntziachristos, *Nat. Med.* **2003**, *9*, 123–128.
[9] A. P. Schaap, M. D. Sandison, R. S. Handley, *Tetrahedron Lett.* **1987**, *28*, 1159–1162.
[10] J. Fan, M. Hu, P. Zhan, X. Peng, *Chem. Soc. Rev.* **2013**, *42*, 29–43.
[11] N. Hananya, A. Eldar Boock, C. R. Bauer, R. Satchi-Fainaro, D. Shabat, *J. Am. Chem. Soc.* **2016**, *138*, 134387–13446.
[12] N. Watanabe, H. Kino, S. Watanabe, H. K. Ijuin, M. Yamada, M. Matsumoto, *Tetrahedron* **2012**, *68*, 6079–6087.
[13] A. P. Schaap, H. Arkhavan-Tafti, WO9007511 A1, **1997**.
[14] B. Valeur, M. N. Berberan-Santos, in *Molecular Fluorescence Principles and Applications*, Wiley-VCH, **2012**.
[15] O. Green, T. Eilon, N. Hananya, S. Gutkin, C. R. Bauer, D. Shabat, *ACS Cent. Sci.* **2017**, *3*, 349–358.
[16] O. Green, S. Gnaim, R. Blau, A. Eldar-Boock, R. Satchi-Fainaro, D. Shabat, *J. Am. Chem. Soc.* **2017**, *139*, 13243–13248.
[17] D. Cao, L. Zhu, Z. Liu, W. Lin, *J Photochem. Photobiol. C Photochem. Rev.* **2020**, *44*, 100371.
[18] Y. J. Gong, X. B. Zhang, C. C. Zhang, A. L. Luo, T. Fu, W. Tan, G. L. Shen, R. Q. Yu, *Anal. Chem.* **2012**, *84*, 10777–10784.
[19] G. Li, T. Hirano, K. Yamada, *Dyes Pigm.* **2020**, *178*, 108339.
[20] J. Han, J. Jose, E. Mei, K. Burgess, *Angew. Chem. Int. Ed.* **2007**, *46*, 1684–1687; *Angew. Chem.* **2007**, *119*, 1714–1717.
[21] H. N. Kagalwala, L. Bueno, H. Wanniarachchi, D. K. Unruh, C. I. Pavlich, K. B. Hamal, G. J. Carlson, K. G. Pinney, R. P. Mason, A. Lippert, *Anal. Sens.* **2022**, *e202200085*.
[22] K. J. Bruemmer, O. Green, T. A. Su, D. Shabat, C. J. Chang, *Angew. Chem. Int. Ed.* **2018**, *57*, 7508–7512; *Angew. Chem.* **2018**, *130*, 7630–7634.
[23] Z. Li, R. Bittman, *J. Org. Chem.* **2007**, *72*, 8376–8382.
[24] X. Zhang, Y. Chen, *Dyes Pigm.* **2013**, *99*, 531–536.

[25] G. Ulrich, R. Ziessel, A. Harriman, *Angew. Chem. Int. Ed.* **2008**, *47*, 1184–1201; *Angew. Chem.* **2008**, *120*, 1202–1219.
[26] E. Pretsch, P. Bühlmann, M. Badertscher, in *Structure determination of organic compounds*, Springer, **2009**.
[27] Z. Gao, X. Zhang, Y. Chen, *Dyes Pigm.* **2015**, *113*, 257–262.
[28] J. Hong, Q. Li, Q. Xia, G. Feng, *Anal. Chem.* **2021**, 16956–16964.
[29] Y. Erande, S. Chemate, A. More, N. Sekar, *RSC Adv.* **2015**, *5*, 89482–89487.
[30] R. Sukato, N. Sangpetch, T. Palaga, S. Jantra, V. Vchirawongkwin, C. Jongwohan, M. Sukwattanasinitt, S. Wacharasindhu, *J. Hazard. Mater.* **2016**, *314*, 277–285.
[31] Y. Zhang, Y. Hao, X. Ma, S. Chen, M. Xu, *Environ. Pollut.* **2020**, *265*, 114958.
[32] T. Gareis, C. Huber, O. S. Wolfbeis, J. Daub, *Chem. Commun.* **1997**, *1*, 1717–1718.
[33] H. Sunahara, Y. Urano, H. Kojima, T. Nagano, *J. Am. Chem. Soc.* **2007**, *129*, 5597–5604.
[34] J. Wang, Y. Hou, C. Li, B. Zhang, X. Wang, *Sensors Actuators B. Chem.* **2011**, *157*, 586–593.
[35] H. Guo, Y. Jing, X. Yuan, S. Ji, J. Zhao, X. Li, Y. Kan, *Org. Biomol. Chem.* **2011**, *9*, 3844–3853.

Manuscript received: November 29, 2022
Revised manuscript received: February 16, 2023
Accepted manuscript online: February 16, 2023